Advances in Colloid and Interface Science 208 (2014) 252–263

Contents lists available at ScienceDirect

Advances in Colloid and Interface Science

journal homepage: www.elsevier.com/locate/cis

Hydrogels from phospholipid vesicles

D. Gräbner [a], H. Hoffmann [a,*], S. Förster [b], S. Rosenfeldt [b], J. Linders [c], C. Mayer [c], Y. Talmon [d], J. Schmidt [d]

[a] University of Bayreuth, BZKG, Gottlieb-Keim-Str. 60, 95448 Bayreuth, Germany
[b] University of Bayreuth, Physical Chemistry I, 95440 Bayreuth, Germany
[c] University of Duisburg-Essen, Institute of Physical Chemistry, S05 R00 L81, Universitätsstr. 2, 45141 Essen, Germany
[d] Technion-Israel Institute of Technology, Dept. of Chemical Eng., Haifa 32000, Israel

ARTICLE INFO

Available online 11 March 2014

Keywords:
Diacylphosphocholin
Vesicles
Gels
Swelling of dispersions

ABSTRACT

It is shown that phospholipid dispersions with a few percent of diacylphosphocholine PC in water can be swollen to single-phase lyotropic liquid crystalline L_α-phases by the addition of co-solvents like glycerol, 1,3-butyleneglycol BG or 1,2-propyleneglycol PG. The birefringent L_α-phases contain small unilamellar and multilamellar vesicles if the temperature of the samples is above the Krafft-Temperature T_m of the phospholipid. When such transparent birefringent viscous samples are cooled down below T_m the samples are transformed into birefringent gels. Cryo-TEM and FF-TEM measurements show that the bilayers of the vesicles are transformed from the liquid to the crystalline state during the transformation while the vesicle structure remains. The bilayers of the crystalline vesicles form adhesive contacts in the gel. Pulsed-field gradient NMR measurements show that two different kinds of water or co-solvent can be distinguished in the gels. One type of solvent molecules can diffuse like normal solvent in a continuous bulk phase. A second type of water diffuses much more slowly. This type of solvent is obviously trapped in the vesicles. The permeability of the crystalline vesicles for water and solvent molecules is much lower in the crystalline state than in the fluid state.

Maximum swelling of the diacylphosphocholin dispersions occurs when the refractive index of the solvent is matched to the refractive index of the bilayers. The attraction between the bilayers is at a minimum in this state and the liquid crystalline L_α-phase's undulation forces between the bilayers push the bilayers apart. On transformation to the gel state the crystalline bilayers assume a high elastic bending rigidity. Undulations of the bilayers are now suppressed, and the bilayers can form adhesive contacts.

Oscillating rheological measurements show that the gels with only 1% of phospholipids can have a storage modulus of 1000 Pa. The gels are very brittle. They break when they are deformed by a few percent.

Contents

* Corresponding author.
E-mail address: heinz.hoffmann@uni-bayreuth.de (H. Hoffmann).

http://dx.doi.org/10.1016/j.cis.2014.02.011
0001-8686/

1. Introduction

The authors are pleased to contribute a manuscript in honor of the 80th birthday of W. Helfrich. They are especially glad that this manuscript is based on a novel hydrogel that has only recently been discovered, and that is completely controlled by the undulation theory of phospholipid bilayers of W. Helfrich [1]. At the discovery of the hydrogels, the origin of the gelation process was not clear. The discovery was due to an accidental observation that dilutes birefringent L_α-phases from diacylphosphocholine (PC) in a water–glycerol mixture turned into a stiff gel when samples with the L_α-phase were cooled down from temperatures above the Krafft-Temperature to temperatures below the Krafft-Temperature [2]. At its discovery, the structure of the PC inside the gel was not clear. With time and with more experimental results from TEM, SAXS and from PFG-NMR the structure became clear, and it turned out that the gel could be understood on the basis of the Helfrich theory [1,2].

In this article some of the old results from ref. [2] are summarized and new results are added to demonstrate that the hydrogels can be produced by different solvents and solvent mixtures. Looking back it is surprising that the gels had not been observed much earlier. This had probably to do with the fact that the many groups all over the world that are working with vesicle phases from PC and with aqueous dispersions of PC were not aware of the fact that the collapsed bilayers, which are present in dispersions, can be swollen by a simple trick to interlamellar spacings up to the range of 100 nm [3]. This was known to one of the authors, and for that reason the group could prepare single L_α-phases with as little as 1% of PC. The discovery of such gels was made when phases had been prepared in the evening at temperature above T_m, around 55 °C. In the morning, after the temperature control system had been switched off for the night, the samples were found to have transformed into stiff transparent birefringent gels [2].

Many results on the properties of bio-membranes and on the interaction of bio-membranes with other molecules are obtained on diacylphosphatidylcholine (PC) vesicles. Such vesicles do not form spontaneously when the phospholipids are dispersed in water. The phospholipids remain in a condensed state with little water in between the hydrated head-groups. When the dispersion is not stirred the particles cream up and a two-phase system develops with the phospholipids forming the upper layer. This situation is true in the liquid or in the crystalline state of the phospholipids.

Vesicles can be prepared from such dispersions by the action of shear forces on the particles that occur in sonication or extrusion processes [4,5]. Vesicles can also be prepared when phospholipids are dissolved in a good solvent, a thin film is formed from the phospholipid solution by vaporization of the solvent, and the film is then dispersed in water [6]. In all these procedures the size of the vesicles depends on the intensity and the duration of the shearing forces, and hence on the history of their preparation. In spite of these difficulties it is possible to prepare vesicle phases with only one bilayer and with small diameters in the range of tens of nm (small unilamellar vesicles, SUV), or vesicles with dimensions of micrometers (large unilamellar vesicles, LUV) [7]. It is furthermore possible to prepare vesicles with several bilayers (multilamellar large vesicles, MLV). We should keep in mind, however, that vesicles which are produced by a mechanical process are not in a thermodynamically stable state. In this respect the situation is very different when vesicles are prepared from surfactants, in particular from mixtures of single chain surfactants [8–10].

As mentioned, PC-vesicles can also be prepared without the use of strong shearing forces simply by adding co-solvents like glycerol or 1,3-butyleneglycol to aqueous dispersions of PC [2]. Experiments demonstrated that the PC-particles can swell by the addition of co-solvents, whereby the bilayers are separated to large distances up to 100 nm.

The resulting L_α-phases can simply be transformed to vesicle phases by a slight stirring of the single phase samples. The previous results were obtained with the co-solvents glycerol and 1,3-butyleneglycol (BG), or mixtures of the two solvents. In this paper, new results were produced with the solvent 1,2-propyleneglycol (PG) and mixtures of PG and glycerol.

2. Experimental section

The PC used was Coatsome NC 21, a hydrogenated soybean phosphatidylcholine from NOF corporation and used without further purification. The PG was from Fluka, Ph Eur quality. The anionic phospholipid was 1,2-dipalmitoyl-sn-glycero-3-phosphate, mono-sodium salt, DPPA-Na, product name LIPOID PA 16:0/16:0 from Lipoid, again used without further processing.

The DSC experiments were done on a Setaram μDSC 3. The experiments were carried out in the usual manner, using the pure solvent mixture as reference. Heating/cooling rate was 0.5 K per min. Sample mass was 300 to 600 mg, equivalent to 6 to 12 mg PC.

All SAXS data reported here were measured using the small-angle-X-ray system "Double Ganesha AIR" (SAXSLAB, Denmark). The X-ray source of this laboratory-based system is a rotating anode (copper, MicoMax 007HF, Rigaku Corporation, Japan) providing a micro-focused beam. The data are recorded by a position sensitive detector (PILATUS 300 K, Dectris). To cover the range of scattering vectors between 0.005 and 2.0 $Å^{-1}$ different detector positions were used. The temperature of the samples was controlled using a Linkam high temperature control stage with a ± 1 °C precision. The measurements were done in 1 mm glass capillaries (Hilgenberg, code 4007610, Germany) at room temperature if not mentioned otherwise. The circularly averaged data were normalized to incident beam, sample thickness and measurement time before subtraction of the solvent.

Rheology was measured on a ThermoHaake RS 600 machine equipped with a TC 81 peltier-based temperature control. We measured in cone-plate geometry with 60 mm cone diameter and cone angle of 1°, in stress controlled mode.

All PFG-NMR-measurements are performed on a Bruker Avance 400 spectrometer (Bruker AG, Karlsruhe, Germany) equipped with a BAFPA 40 gradient amplifier and a Bruker DIFF30 probe. The instrument is tuned to 400 MHz proton frequency, gradient pulses are adjusted to gradient strengths between 5 and 550 G/cm with individual durations of 2 ms. For all measurements, the stimulated echo (90°-τ_1–90°-τ_2–90°-τ_1-echo) is used in combination with the gradient pulses during each τ_1 waiting period. The duration of the 90°-pulses is 9 μs, the waiting period between the 96 repetitions (scans) of each experiment amounts to 5 s. The spacing Δ between the two gradient pulses is varied between 50 ms and 400 ms. The temperature of the sample is adjusted in a constant gas flow, the absolute temperature setting in the probe is checked with a separate ethylene glycol sample.

The free induction decays resulting from the addition of each set of 96 experiments were Fourier transformed and analyzed for the echo signal decay vs. the gradient strength G and the pulse spacing Δ. Characteristic signals were chosen for the observation of individual system components. For the analysis of the diffusion profile, the relative signal intensities I/I_0 (I_0 referring to the signal intensity at gradient strength $G = 0$) are plotted logarithmically vs. the parameter $\gamma^2G^2\delta^2(\Delta - \delta/3)$, with γ being the gyromagnetic ratio of protons, G the strength of the pulsed field gradient, δ and Δ the duration of and the spacing between the two gradient pulses.

Cryogenic transmission electron microscopy (cryo-TEM) specimens were prepared in a controlled environment vitrification system (CEVS), to preserve the native structure of the system [8]. A drop of the solution was placed on a carbon-coated perforated polymer film, supported on a 200 mesh TEM copper grid, mounted on a tweezers. Thin liquid films (preferably less than 300 nm thick) were formed by blotting excess solution with a metal strip wrapped with a filter paper. In the case of the presence of a gel at the required temperature, the specimen was warmed up to a temperature at which it is liquid, prepared in the CEVS at that temperate, and cooled at controlled saturation conditions to the required gel temperature. The thin liquid specimen was then plunged into the proper cryogen, liquid ethane at its freezing point (−183 °C) for dispersions in water, and liquid nitrogen at its boiling point (−196 °C) for PG containing mixtures. Although liquid nitrogen is a relatively poor cryogen (compared to liquid ethane at its freezing point), it can still vitrify PG containing specimens, without leaching out the organic component, as liquid ethane may do [9].

We performed cryogenic transmission electron microscopy (cryo-TEM) imaging with an FEI Tecnai T12 G^2 electron microscope, operated at an accelerating voltage of 120 kV. The cryo-specimens were transferred under controlled conditions into a Gatan 626DH cryo-holder, using its "transfer station", and equilibrated in the TEM below −178 °C. We examined the specimens in the low-dose imaging mode to minimize electron-beam radiation damage. We recorded the images digitally by a Gatan US1000 high-resolution cooled CCD camera, using the Gatan DigitalMicrograph software.

3. Results

3.1. The swelling of PC dispersions by co-solvents

Many organic solvents are completely miscible with water. They can be used to modify the unique properties of water. Organic solvents are added to aqueous phases for different reasons. Sometimes, solvents like tetrahydrofuran are added to increase the solubility of hydrophobic compounds like block copolymers [11]. In addition to increasing the solubility, such solvents also change the self-aggregation behavior of surfactants and block copolymers. In many such situations the addition of the solvent increases the critical micelle concentrations (CMC) dramatically, and the hydrophobic compound may no longer form micelles, when large amounts of the solvent, 10% or more, are added. The self-aggregation process can simply be turned on again in such situations by adding water. This procedure has been used in the past for the preparation of vesicles with block copolymers. Conversely, protic solvents like glycerol and glycol have little effect on the CMC of surfactants and lipid molecules [12]. It is for this reason that glycerol can be added to the samples in the preparation of cryo-TEM micrographs. On quenching the specimen to low temperatures, 10% addition of glycerol prevents the formation of ice crystals, which could destroy micellar structures, but the glycerol doesn't affect the sample micellar structures.

Glycerol has very little effect on the hydrophobic interaction between surfactants and the solvent, even when the glycerol content is increased up to 50%. This effect is best known by the fact that the semen of bulls can be stored for a long time in mixtures of water and glycerol at low temperature and the activity of the semen is not lost. After heating the semen samples to room temperature, the semen can still be used to fertilize the eggs of cows. Obviously, the delicate structure of the semen cells is not destroyed by this drastic change of environment, and the semen can be revived to life.

On the molecular level, the addition of co-solvents to water can change the solubility of amphiphiles, their hydrophobic interaction, CMC and the intermicellar interaction.

At 1.33 the solvent water has a low refractive index, but a high dielectric constant. Organic co-solvents have higher refractive indexes in the range of 1.4 to 1.5, and dielectric constants much lower than that of water. As a consequence the repulsive and attractive forces between micelles or bilayers are changed, even when the added co-solvents have little effect on the CMC of the aqueous systems.

This effect can best be demonstrated by the addition of glycerol to samples in which an L_1-phase is in equilibrium, but macroscopically separated from an L_α-phase. With increasing glycerol concentration the volume fraction of the L_α-phase increases until the sample is in a single L_α-phase [13]. This effect was first demonstrated on the phase diagram of an ABA block copolymer of dimethylsiloxane with poly(ethylenglycol) [3]. Later experiments on other two-phase L_1/L_α systems confirmed that result as a general behavior [13]. It can even be extrapolated to dispersions of phospholipids in water. In the dispersions, the bilayers of the phospholipids are present in the condensed state. They attract each other and squeeze out the water. Parsegian had already observed that the interlamellar spacing between bilayers swells somewhat when glycerol is added [14]. He did not realize however that the dispersions can be swollen to L_α-phases with interlamellar spacings as large as 100 nm. This has been accomplished only recently in experiments with diacylphosphatidylcholin in solvent mixtures of water–glycerol and in mixtures of glycerol and 1,3-butyleneglycol. Dispersions of the phospholipid with as little as 1% could be swollen to single L_α-phases [2].

The swelling of the particles can be understood on the basis of the Hamaker constant, H, that controls the attraction of the bilayers

$$H \propto \frac{(n_b - n_s)^2}{(n_b + n_s)^{3/2}} \quad (1)$$

n_b is the refractive index of the bilayers, and n_s is the refractive index of the solvent.

With increasing glycerol concentration the refractive index of the solvent increases, at around 60% glycerol the refractive index of the solvent matches the refractive index of the bilayers. At that point the attraction between the bilayers vanishes [2]. The effect can only be active if the bilayers can undulate, that is if they are in the liquid state. It is noteworthy that the effect occurs not only with protic solvents like glycerol but also with aprotic solvents like dimethylsulfoxide. All these additives have little effect on the CMC of the compounds, but they change the refractive index of the solvent. The effect is also visible in aqueous phase diagrams of non-ionic surfactants when increasing amounts of water are replaced by glycerol [15]. At constant temperature the two-phase situation in L_1/L_α situations is transformed to single-phase L_α-phases with increasing glycerol content.

In this investigation it will be demonstrated that besides the solvent 1,3-butyleneglycol (BG), the solvent 1,2-propyleneglycol (PG) can be used to cause swelling of PC particles.

The similarity of the solvents PG and BG with regard to the solution behavior of PC can best be demonstrated by visual inspection of the samples. Only the PC samples in PG are shown here because samples of PC in BG were already shown previously [2].

3.2. The formation of hydrogels by cooling L_α-phases of PC

Fig. 1a shows six samples of PC in PG and partly with water at 60 °C. These samples as well as another series of samples with increasing content of anionic phosphocholine were used for the investigations described in this publication. In the first three samples the concentration of PC in pure PG was varied from 1% to 3%. In the following we refer to this series as A-series.

The samples of the A-series are of low viscosity, transparent and optically isotropic at 55 °C. Under flow, the samples furthermore do not show any sign of flow birefringence. These properties indicate that the samples contain no vesicles and no threadlike micelles. Samples in BG behaved the same way. At 55 °C the samples seem to contain molecular solutions of PC in PG. As will be shown later, this will be in agreement with the results of SAXS, PFG-NMR and cryo-TEM. At room temperature

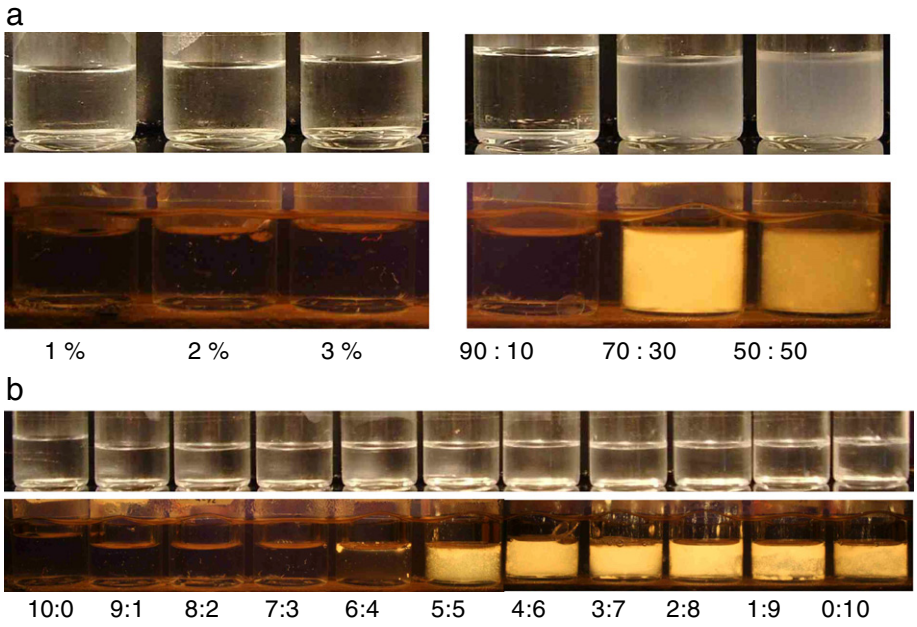

Fig. 1. a: left: PC in PG with increasing concentration (A-series); right: 3 wt.% PC in mixtures of PG and water (ratio given below, B-series). Top row in direct light; bottom row: between crossed polarisors. All photos at 60 °C. b (D-series): 3 wt.% PC in mixtures of PG with glycerol (PG/glycerol mixing ratio given below the samples). Top: direct light; bottom: between crossed polarisors. All photos at 60 °C.

all three samples are stiff, birefringent gels that are slightly turbid (see Fig. 3a).

The next three samples contain 3% PC in PG with 10%, 30% and 50% of water (B-series). At 55 °C they are transparent at low water content and become increasingly turbid with increasing water content. At 10% water, the sample is still isotropic, but at higher water content, the samples become birefringent. The B-series samples are more viscous than the samples in the pure solvent. The addition of water to the PG has caused the formation of vesicles and multilamellar vesicles. It should be noted that all three samples are in a single-phase state with only 3% of PC. Assuming the simple model of ideal lamellaes (L_α-phases) this means that the interlamellar spacings between the bilayers of the vesicles must be 33 times (e.g. 100/wt.%) larger than the thickness of a bilayer, which is in the range of 5 nm. The spacings must therefore be in the range of (100/wt.%) ∗ bilayer thickness, e. g. for 3% ca. 167 nm. Note that we haven't observed such a correlation length in SAXS experiments, even not if we increased the PC content to 12%. On cooling to room temperature the samples of the B-series were transformed to birefringent gels. As can be noted from the photos, the textures of the birefringence of the samples in the liquid, and in the gel state are somewhat different. The birefringent gels at room temperature are transparent.

When more than 50% water is added to the PG samples, they loose their single phase character, and turn into macroscopically separated two-phase systems: one birefringent PC phase, and one low viscosity solvent phase.

Obviously, with more water the attraction between the bilayers becomes stronger, the spacings between the bilayers become smaller, and the MLV phase contracts to a separate phase with excess solvent. The contraction can be prevented when water is replaced by glycerol. Stable single-phase PC samples can be formed in glycerol/PG mixtures as is shown in Fig. 1b.

These results indicate that the strategy which has been used for the formation of vesicles from block copolymer can also be used to form vesicles from phospholipids: the phospholipid can first be dissolved in a good solvent that is miscible with water, and in which the phospholipid is soluble as single molecules [10]. Then the good solubility of the phospholipid chains is reduced by the addition of water, until the phospholipid begins to aggregate.

It remains to be seen whether gels can also be formed by this strategy in other solvent mixtures.

In the C-series, increasing concentrations of an anionic phospholipid (DPPA with a small counterion like sodium) were added to a sample of 3% phospholipid in a mixture of 70% PG and 30% water. It was hoped that by introducing the anionic phospholipid a repulsion between the vesicles is generated, which suppresses the formation of the gels. Unlike expected, turned bottle experiments showed still gel-like behavior. In the SAXS patterns even more defined correlations were obtained (cf. Fig. 6a).

The results in Fig. 1a and b at 60 °C show that the solvent 1,2-propyleneglycol (PG) has similar properties as the solvent 1,3-butyleneglycol (BG). From visual inspections it seems that single L_α-phases can already be obtained with 1% of PC in PG/water mixtures. We have to admit that SAXS-measurements of PC in mixtures of 70%PG and 30% water (up to 12% PC) haven't shown the expected correlation peaks at 65 °C. The reason for this observation is still unclear. Note, however, that we obtained the L_α-phase at 45 °C. Up to now, data for the temperature range in between don't exist. Single L_α-phases can also be obtained in mixtures of PG with glycerol as shown in Fig. 1, similar to the situation in mixtures of BG with glycerol, which were shown previously. All the phases with different mixing ratios of the two solvent mixtures, e.g. PG/glycerol and BG/glycerol, show a strong stationary birefringence, a typical feature of the L_α-phase. The birefringence patterns in the samples in PG/glycerol, however, vary somewhat. This is not surprising, because the samples had not been prepared under constant shearing conditions. The samples were simply mixed with a vortexer. Previous measurements on L_α-phases from surfactants had shown that L_α-phases are always transformed to multilamellar vesicle phases with shear. The number of bilayers in the MLVs depends on the shear rate and the time of shearing [16–18]. In this paper no effort was made to check the exact relation between the size of the vesicles and the shear condition. We simply assume that the L_α-phases produced by vortexing the samples contain both MLVs and SUVs.

In Fig. 2 the refractive index and the surface tension of mixtures of glycerol with 1,3-butyleneglycol (BG) are plotted against the composition. It is to be assumed that the corresponding diagram with PG is very similar, as the refractive index of PG is only 1.432 (Fluka/SigmaAldrich),

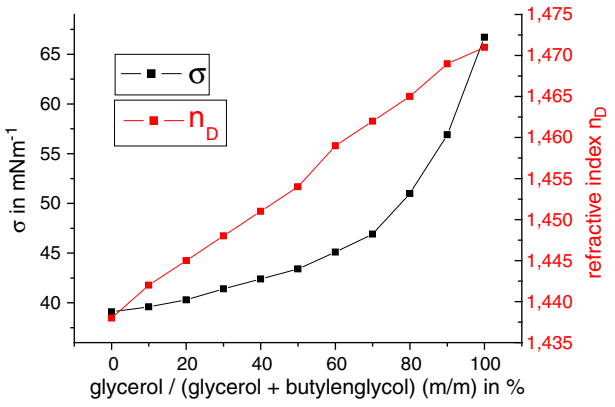

Fig. 2. Surface tension and refractive index n_D of glycerol/butyleneglycol as a function of the mixing ratio at 25 °C (n_D: λ = 590 nm).

compared to the value of 1.439 for BG. The surface tension of PG is 36 mN/m [20] compared to 39 mN/m for BG. As the refractive index is assumed to be the key property of the solvent that controls the structure of the samples, replacing BG with PG as solvent probably only means that a slightly higher content is needed – e. g. in mixtures with glycerol – to achieve the same refractive index of the solution mixture and therefore the same sample behavior. Fig. 2 shows that all the mixtures have a refractive index that is higher than the refractive index of hydrocarbons and the bilayers of the PC in the L_α-phases. This is important for the swelling of the phases. The surface tension of BG is 39 mN/m, somewhat lower than the one for glycerol with 65. This parameter is probably relevant for the quantitative hydrophobic effect of the solvent. It will not be studied quantitatively in this paper.

It is general knowledge that surfactant solutions can sometimes be cooled below the Krafft-temperature of the surfactant for long periods of time (days), while the surfactant does not precipitate. The supercooled solutions are in a thermodynamically metastable state. The formation of nuclei is necessary for the precipitation. The situation is very different for the liquid L_α-phases of PC. The samples gel as soon as the L_α-phases are cooled below the Krafft-temperature of the PC and thereafter seem to be in a thermodynamically stable state.

Even at small concentration of the PC, the gels are stiff enough to be turned upside down, without observed flow. On cooling below the temperature of the melting transition, T_m, the samples become slightly turbid as is shown in Fig. 3a.

Upon cooling the PC molecules are transformed from the liquid state to the crystalline state. This conclusion brings up the question what process is responsible for the gelation. The answer will be discussed in the chapters on the experimental results and the macroscopic properties of the gels that were determined by cryo-TEM, FF-TEM and SAXS.

3.3. DSC investigations

In this section we present results obtained from systems with BG/glycerol instead of PG/glycerol mixtures. It will be shown that the change of the solvent has a moderate influence on the gelation temperature. DSC experiments were carried out on samples containing glycerol and BG instead of PG to determine the exact melting temperatures of the gels. It is interesting to note that the Krafft-temperature of the PC depends somewhat on the mixing ratio of the two solvents. The melting temperatures correlate nicely with the mixing ratio of the solvents for the heating curves. It goes down from 55 °C in pure glycerol to 50.5 °C in 20% glycerol/80% BG.

The molar melting enthalpies are slightly higher than usual for aqueous systems, where typically 20 to 40 kJ mol^{-1} were found [19].

Surprisingly, in contrast to the melting temperatures, the enthalpies do not correlate with the mixing ratio of the solvents.

The values for T_m shown in Table 1 are the onset temperatures. Onset temperature is determined by drawing the tangent to the graph's inflection point, i. e. where the graph is steepest and has maximum negative slope, and intersecting that tangent with the extrapolated baseline. These onset temperatures are preferred over the temperature of the maximum of the signal, as the onset is, e. g., independent of the heating rate, which is not necessarily the case for the maximum of the signal.

Note that for the determination of the thermodynamic melting point, only the heating curves can give reliable results, as the gelation tends to be delayed due to supercooling. The supercooling range depends also on the mixing ratio. It was the largest, 7 °C, for the 8:2. The appearance of two recrystallization peaks at high glyerol contents in

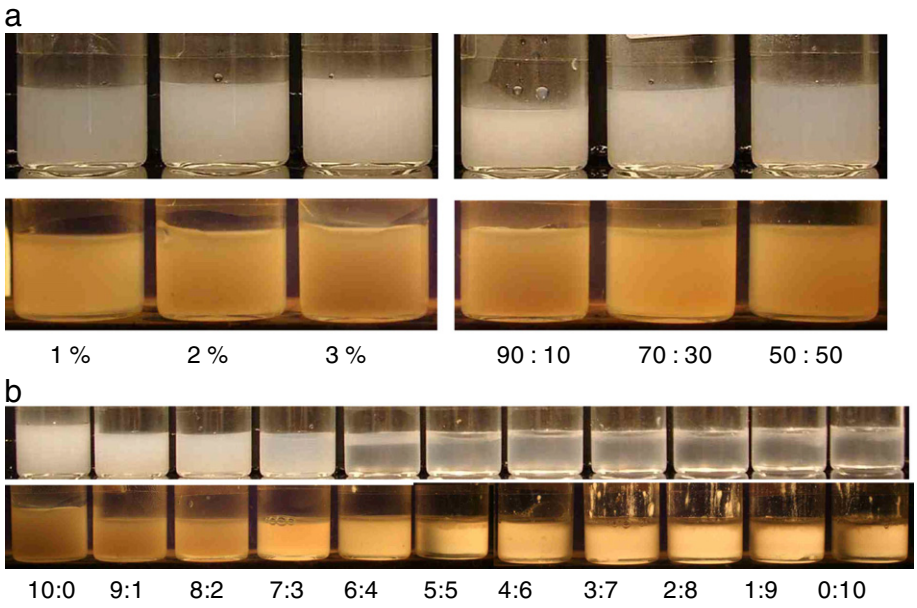

Fig. 3. a: samples from Fig. 1a at room temperature; left: PC in PG with increasing concentration (A-series); right: 3 wt.% PC in mixtures of PG and water (ratio given below, B-series). Top row in direct light; bottom row: between crossed polarisors. b: samples from Fig. 1b (D-series, i. e. 3% PC in PG/glycerol; PG/glycerol mixing ratio given below the samples) at room temperature; top: in direct light; bottom: between crossed polarisors.

Table 1
Melting temperatures T_m (onset) and molar melting enthalpies $\Delta_m H$ for gels from 2 wt.% PC in glycerol/BG at different mixing ratios.

Glycerol:BG ratio	T_m in °C	$\Delta_m H$ in kJ mol^{-1}
10:0	54.0	52.1
8:2	52.8	43.5
5:5	51.4	51.8
2:8	50.5	44.8

Fig. 4 is not sufficiently explained so far; maybe it is related to the fact that the investigated PC consists of two components with slightly different hydrocarbon chain lengths.

The question is why the system forms two-dimensional crystals as will be shown later, not three-dimensional crystals when the samples are cooled below T_k. This has probably to do with the low concentration of PC in the monomer state, and consequently with the low exchange rate between the bilayers and the bulk phase. While the CMC was not measured, it is likely that it is below 10^{-10} M, because of the two large hydrophobic groups in PC.

For this reason there is not enough monomer material available for being delivered for the formation of nuclei of three-dimensional crystals when $T < T_k$. The system has therefore no choice but to form two dimensional crystals. Only small deformation of the molecules in the bilayers is necessary for that process.

3.4. Conductivity results

To obtain information on the continuity of the solvent phase and on the network phase of PC, we measured the conductivity of the samples. 100 mM NaCl was added to the samples for this purpose. The conductivity was measured with and without PC. The L_α-phases above T_m have a conductivity that is on average at least a factor 2 lower than the solvent mixtures without PC. This effect can be expected and is usually explained by the entrapment of solvent and hence NaCl in the MLV. The entrapped NaCl cannot contribute to the conductivity of the samples. Only NaCl that is contained outside of the MLVs in the continuous phase may on first approximation determine the conductivity. A factor of two between the conductivity would thus indicate that the volume fraction of the continuous phase makes up about 50%, a reasonable value for densely packed vesicles.

If we assume further that on the sol/gel transition the bilayer is just transformed from the liquid to the crystalline state, and no other process occurs, the conductivity would not be expected to change very much. Part of the ions would remain in the continuous solvent phase and, could diffuse as fast as in the liquid state. However, when the conductivity is measured at the sol/gel transitions, a large change of almost one order of magnitude is observed (Fig. 5).

Obviously, one more process must occur during the gelation. It is likely that this process is the formation of a three-dimensional network of the vesicles. When the vesicles are transformed into the crystalline state, the bilayers become stiffer, and the undulation of the bilayers is suppressed. The vesicles should therefore switch from a repulsive to an attractive interaction, and they form adhesive contacts. This applies also to the innermost vesicles in the MLVs. As long as the bilayers are in the liquid state, the interlamellar distance between the bilayers is about the same. In SAXS or SANS measurements this uniformity of the interlamellar distance gives rise to a correlation peak that has been observed for many vesicle systems [21]. In SAXS experiments an MLV can be considered as a piece of an L_α-phase. The formation of the contact between vesicles inside one large onion (MLV) should not affect the conductivity of the system. It would however affect the scattering behavior of the system. The order in the system caused by the undulation forces disappears. The formation of the contacts between the outermost bilayers of the vesicles must have a strong influence on the conductivity. The contacts block the pathway of the ions in the continuous part of the phase. This would reduce the conductivity, as indeed we found experimentally (Fig. 5). While a theoretical model for such a situation does not seem to be available for the quantitative discussion of the results, the large jump seems surprising. The permeability of small ions through vesicles in the liquid state was found to be low in other systems; such ions inside the vesicles, therefore, cannot make considerable contributions to the total conductivity. If this were true also for our system, the sharp rise in conductivity that occurs upon melting might have other reasons. It is conceivable that the vesicles in our system rupture or get holes when the gels melt.

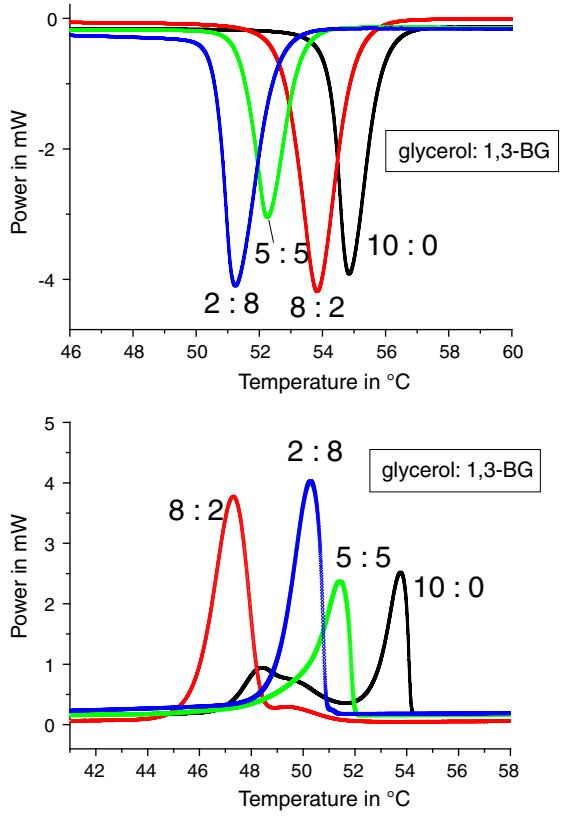

Fig. 4. DSC curves for 2 wt.% PC in glycerol/BG mixtures at different mixing ratios. Top: heating curves (endothermic peaks); bottom: cooling curves (exothermic peaks). Note that the samples were prepared with the BG, not with PG.

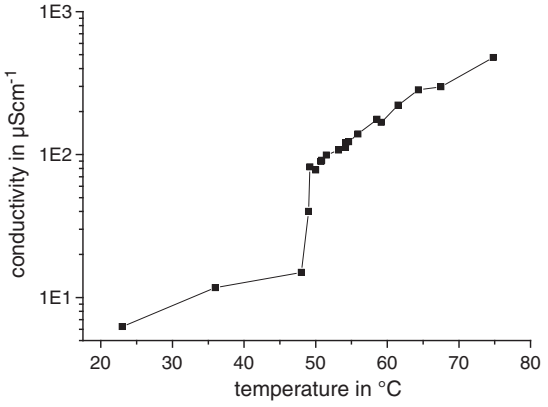

Fig. 5. Conductivity of 2% PC in glycerol/1,3-butyleneglycol as a function of temperature (100 mM NaCl added to obtain sufficient bulk conductivity). Note, again, that the second solvent was not propyleneglycol but butyleneglycol.

3.5. Small-angle X-ray scattering

3.5.1. Results and discussion

All PC samples, which we investigated by SAXS showed stationary birefringence at 25 °C. Thus, we expected large multi-lamellar vesicles, in which the bilayers are separated by solvent molecules. In SAXS such an L_α-phase appears as lamellar phase and can be identified by peaks in the ratio 1:2:3:4… At room temperature the samples were gel and at 65 °C fluid-like. These samples were measured in a temperature series of 25 °C, 45 °C, 65 °C and again 25 °C. The SAXS measurements showed two different types of data: one for the gel-like samples (25 °C, 45 °C) and one for the fluid-like samples at 65 °C. Note that the results of 25 °C heating up, 45 °C and 25 °C heating down were identical.

In Fig. 6a characteristic SAXS patterns for intermediate concentrations of PC in the solvent mix 70% propylenglycole-30% water are shown. As expected for the gel a lamellar phase was obtained. Note that we obtained experimentally the Bragg peaks corresponding to an interlamellar distance up to hkl values of d_{004}. Independent of the concentration, the Bragg peaks could be described by a unit cell of a

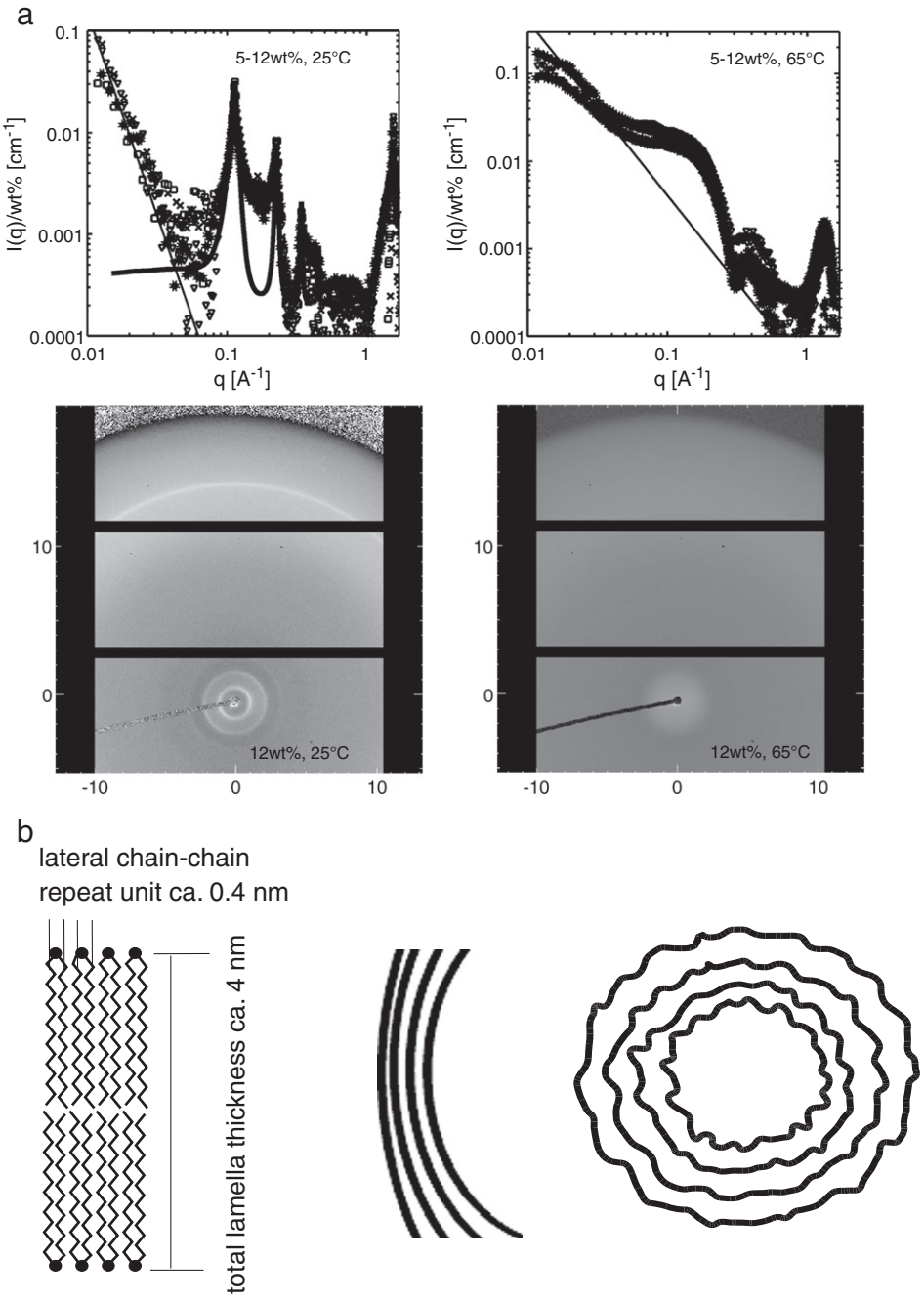

Fig. 6. a: Typical SAXS patterns for intermediate concentrations of PC in the solvent mix 70% propylenglycole-30% water at different temperatures (E-series). The radial averaged intensities belong to 5%, 8%, 10% and 12% PC. Additionally, for the 1D-data at 25 °C a theoretical intensity based on the crystal lattice of simple lamellae and a q^{-4} power law line of huge objects are plotted. In the case of the samples at 65 °C, the scaling of the line is proportional to q^{-2}. b: Sketch of the vesicles and of bilayers in the L_α-phase. Left: Scheme of a bilayer. Middle: L_α-state (25–45 °C). Right: Vesicles in uncondensed state, which are present at 65 °C. c: Characteristic SAXS patterns for PC sample at 25 °C. The A-series denotes the scattering data for different concentrations of PC in propyleneglycol (1–3% PC; the solvent scattering is subtracted). The line corresponds to a q^{-2} power law, which is typical for bilayers. The sample A3 is 3 wt.% PC in propylengylcol. B2 consists of 3% PC in the solvent mix 70% propylenglycole-30% water. C3 is 3%PC in 70% propylenglycole-30% water, where the phosphatdiylcholine membranes have been charged with an anionic phospholipid (PC/DPPA-Na 100:10).

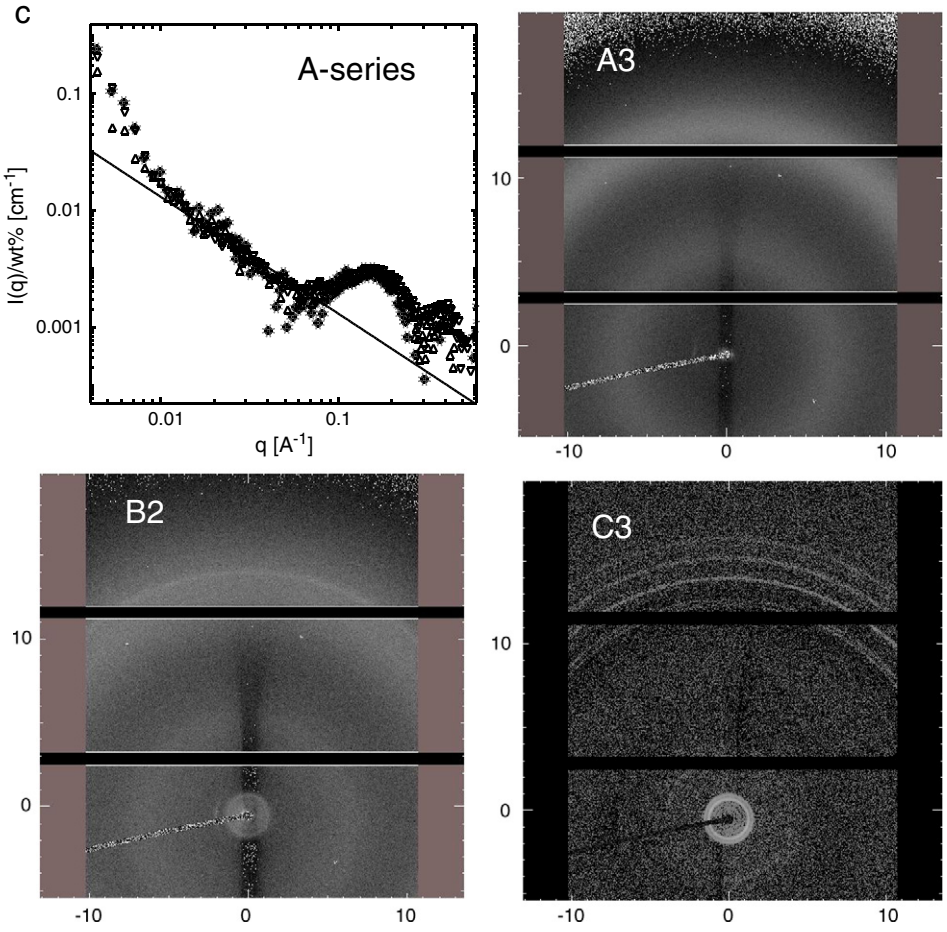

Fig. 6 (*continued*).

lamellae lattice of 5.5 nm and domain size of 30 nm. The value of 5.5 nm can be explained by vesicles, in which the bilayers are only separated by a thin layer of solvent. It's likely that the upturn in the scattering intensity for scattering vectors $q < 0.5\ nm^{-1}$ results from the interparticular structure of the condensed MLV itself. A further characteristic for an L_α-phase is the sharp peak in the wide angle regime, which corresponds to a distance of 0.41 nm. This correlation arises from the ordering of the PC-headgroups in the hk-plane and the ordering of the hydrocarbon chains in the crystalline state. This model is supported by the results of TEM measurements.

At 65 °C the SAXS patterns have changed compared to 25 °C. The q^{-2} power law at low q is characteristic not only for bilayers, but also for other 2D-objects like disks. SAXS-data, however, are consistent with thin disks of only ca. 2 nm. Disk-like micelles of phospholipids can become as thin as this only when heavy interdigitation of the hydrocarbon chains occurs. We suspended the disk model due to the fact that the positions of the minima and the width of the oscillations suggest small disks. This case as well as sufficiently thin PC disks are seldom reported. Besides, the small disks cannot explain birefringence, as only disks with a big diameter or rather a high aspect ratio can be expected to orient spontaneously.

Thus, we assume still a multi-lamellar vesicle phase. At high temperatures the head groups of the PC are more disordered, which results in a broad peak in the wide angle region around 0.45 nm. The aliphatic chains are more flexible. Hence, the condensed state of the bilayers is unlikely and we suggest that due to undulation forces the bilayers of vesicles prefer a swollen state, which is more symmetric [21]. We expected that a swollen L_α-phase should show also sharp Bragg peaks due to the bilayer structure [21], but only a weak broad shoulder in the intermediate q-range, e.g. about distances of 4.5 nm were obtained experimentally. The reason may be a temperature induced movement of the aliphatic chains which hinders the swollen system to order them in fixed positions. But we admit that other phases can't be ruled out. Fig. 6a gives a schematic of the obtained SAXS results for this E-series.

Preliminary SAXS experiments were also done for the series A–C at 25 °C. These samples were birefringent. Thus, L_α-phases are likely for all. The PC was dissolved in PG in the A-series, in a PG–water mix for the B-series and the C-series is 3% PC in a 70% propylenglycole-30% water mix, in which a small amount of an anionic PC was dissolved. In Fig. 6c SAXS data for PC samples in the different surroundings are plotted.

For PC in pure PG, we obtained a similar situation as already discussed above for the E-series at 65 °C. The upturn at lowest q may result from the presence of large objects. The position of the broad shoulder at intermediate scattering vectors is only slightly shifted to dimensions of around 4 nm. Again, no dependence on the concentration was detected.

3% PC in different solvent mixtures with a different PG to water content were investigated in the next sample series. The peak at 0.4 nm in the WAXS regime becomes more pronounced with increasing water content, showing an increasing ordering of the PC headgroups. For this series, even for the sample with 30% water content, sharp oscillation due to the bilayer thickness were hard to obtain. There was a broad rippled shoulder in the expected range of about 4–5 nm, but the peakedness was not pronounced enough for a determination of the unit cell of a lamellae lattice. This feature can be explained by the low concentration of PC.

For the C-series, increasing concentrations of an anionic phospholipid were added to 3% PC in the solvent mix 70% PG-30% water. It was

hoped that the anionic phospholipid (DPPA-Na) introduces a repulsion to suppress the gel-like lamellae state at 25 °C. But the contrary was the case. Around a ratio of PC/DPPA-Na of 100:4, the data suggest the formation of lamellar phases. At that PC/DPPA-Na ratio the data could mainly be described by a lamellae lattice model.

By visual inspection, the sample was a two phase system, due to repulsion of the water. Ca. 5 to 10 vol.% of a clear, low viscous liquid were found at the top of the samples at room temperature. This could be a further indication for the presence of bilayers, which are only separated by a thin layer of solvent molecules. We think that the condensation of the bilayers upon cooling to room temperature is even more pronounced for the sample C3 (PC/DPPA-Na 100:10), which has expelled the water. At this high DPPA-Na content the scattering pattern shows many sharp diffraction peaks, in the SAXS and in the WAXS regime, see Fig. 6c.

A possible explanation may be that the lamellar phase reaches a state where the molecules are in fixed positions. The detailed evaluation of this series is still in progress. So far, several rather broad peaks around 5 nm and several sharp peaks in the WAXS from 0.35 to 0.5 nm were found.

3.6. Rheological results of the gels

In previous measurements it was already shown for a few samples that the storage modulus of the gel samples was very high for dilute samples. For 10% PC samples the storage modulus was in the range of 10,000 Pa. It increased moderately with the oscillating frequency, a feature that is often observed with gels. This feature is a result of the properties of the network. For higher frequencies more elastic network points contribute to the network strength, while they can relax for low frequencies. With increasing temperature the storage modulus decreased somewhat when T_m was approached, but then dropped 4 orders of magnitude at T_m. The result is direct evidence that the gelation is due to the crystallization of the PC in the bilayers.

In this chapter we present rheological results on the gels that reveal detailed properties of the gels that are of general interest. One question is 'how does the storage modulus depend on the concentration of the additive, in our case on PC'? Measurements were therefore made on samples with four different concentrations. All samples were prepared in the same way and the values of the storage moduli are given in Table 2 for the same frequency. The storage moduli increase about linearly with increasing concentration. It would be interesting to compare samples of the same concentration, but for which the shear history of the samples is different. However, such measurements are not available at present. It is known that the average size of MLV decreases with increasing shear rate [22]. It is therefore conceivable that the storage modulus of the gels increases with the shear rate at which the samples were prepared.

Another question is 'how do the storage moduli depend on the solvent composition for the same PC concentration'? In our model the storage moduli should depend on the strength of the binding energy between the vesicles. When the solvent composition is varied, the solvation of head-groups is changed, and that should change the adhesion energy between the vesicles and hence the strength of the network. In Table 3, storage moduli are given for samples that have the same concentration, but different solvent compositions. As noted from the results, the moduli change by about an order of magnitude when the solvent composition is varied.

Table 2
Storage modulus G′ as a function of the PC concentration in a mixture of glycerol:BG 5:5 at room temperature. Note that these samples were prepared with the 1,3-butyleneglycol, not with 1,2-propyleneglycol.

wt.% PC	G′ in Pa at 1 Hz & 5 Pa stress
2.5	1561
5	6683
10	4216
15	7543

Table 3
Storage modulus G′ of the gels from 10% PC in glycerol/BG mixtures with different solvent mixing ratios at room temperature. Again, these samples were prepared with the BG, not with PG.

Mixing ratio glycerol:1,3-BG	G′ in Pa at 1 Hz & 5 Pa stress
10:0	9619
8:2	2264
5:5	5360
2:8	4216

There are considerable changes in the moduli when the solvent mixing ratio is changed, despite the fact that both solvents are quite similar (three carbon atoms with three hydroxy groups compared to four carbons with two hydroxy groups). The values differ by a factor of up to four, though there is no clear correlation between the solvent mixing ratio and the value of the storage modulus. As of now, we cannot rule out completely some remaining effect of the history of the samples.

An interesting property of gels is how much they can be deformed before they break. Some gels break like glasses, and the modulus does not recover, when the samples are kept for longer times. In other gels the strength of the network recovers with time, after the network was broken.

In Fig. 7 results are shown where under oscillating condition the amplitude of the deformation was increased. The result shows that the gels can only be deformed to 1% before the modulus decreases with increasing amplitude. The breakdown of the modulus is irreversible. This result is surprising. It shows that the contacts between the vesicles do not recover after they have been broken. We did not investigate whether there might be a recovery with very long relaxation time.

This result offers the interesting perspective that samples with different rheological properties can be prepared from the gels by breaking the network with oscillating amplitudes with different deformations. It is conceivable that clusters of different sizes are produced by the shear oscillation.

3.7. PFG-NMR-measurements

To elucidate the molecular mobility inside the various hydrogels, pulsed field gradient nuclear magnetic resonance spectroscopy (PFG-NMR) is applied. The free induction decays resulting from the addition of each set of 96 experiments are Fourier transformed and analyzed for the echo signal decay vs. the gradient strength G and the pulse spacing Δ. The methyl signal at 1.150 ppm is chosen for the observation of the self-diffusion of propylene glycol. For the analysis of the diffusion profile, the relative signal intensities I/I_0 (I_0 referring to the signal intensity at gradient strength $G = 0$) are plotted logarithmically vs. the

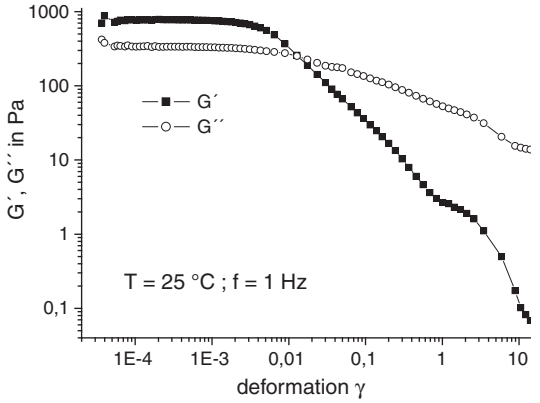

Fig. 7. Oscillating rheological experiment on 3% phosphocholine in 100% glycerol.

parameter $\gamma^2G^2\delta^2(\Delta - \delta/3)$, with γ being the gyromagnetic ratio of protons, G the strength of the pulsed field gradient, δ and Δ the duration of and the spacing between the two gradient pulses. Under these conditions, a free diffusion leads to a linear plot with a slope equal to the negative self-diffusion coefficient [23].

In our given case, these measurements are used to determine the diffusion coefficient of PG in the L_α-phase and in the gel state. In both states, solvent molecules both inside of the vesicles and outside of the MLV are present. It was already shown by previous measurements that the two states of solvent molecules could indeed be distinguished by the PFG-method [24]. One fraction of the molecules showed free diffusion like in the solvent without the PC while the other part showed a much slower (hindered) diffusion. Obviously the second fraction of molecules is entrapped inside the vesicles.

3.8. Systems based on PG as single solvent, samples A1, A2 and A3

More NMR-measurements were now made on the systems with pure PG as the solvent. As expected, two types of solvent molecules were observed in the gel state: one in the free state and one in the entrapped state. However, in the L_α-phase at $T > T_m$ (samples A1–A3 in Table 4, and upper graph in Fig. 8), only one single fraction of solvent molecules can be observed. Further, with self-diffusion coefficients around 1.7 10^{-10} m^2 s^{-1}, the mobility of the PG molecules comes close to the self-diffusion rate of the pure solvent. When these PC/PG mixtures were inspected between crossed polarisors, they appeared dark and did not exhibit any traces of birefringence. It seems therefore that, in the absence of water, the PC does not form vesicles.

In addition, the measurements indicate that the samples in pure PG do not contain micelles. This result is in agreement with the previous results in the PC solutions in the pure solvent BG. These samples were also optically isotropic and did not show any evidence of micellar structures. It thus can be concluded that both solvents PG and BG are very good solvents for PC and that PC is dissolved as individual free molecules and not as micelles. This result is in agreement with the SAXS and TEM measurements where no evidence for micelles could be found.

3.9. Systems based on PG/water mixtures, samples B1, B2 and B3

The result changes dramatically when a sufficient amount of water is added to the solvent. While a solvent mixture of PG/water in a 90:10 ratio still shows a single solvent fraction, a clear separation is found at 70:30 ratio (Fig. 8, bottom), and, to a similar extent, at the of 50:50 ratio (data not shown). At the 70:30 ratio, rapid self-diffusion (D_{app} between 63.6 10^{-12} m^2s^{-1} and 158 10^{-12} m^2s^{-1}, see Table 4, sample B2)

Table 4
Diffusion coefficients from PFG-NMR for the three sample series investigated at T = 55 °C.
A1–A3: 1, 2 and 3% PC in PG; B1–B3: 3% PC in PG water mixtures 90:10, 70:30 and 50:50, resp.; C1–C3: 3% PC in 70% PG/30% water with 0.06, 0.12 and 0.3% of additional anionic phospholipid. The values for Δ denote the spacing between the two gradient pulses varied between 50 and 400 ms.

	Self diffusion coefficients of PG in 10^{-12} m^2 s^{-1}							
	Mobile fraction[a]				Immobile fraction[b]			
	50 ms	100 ms	200 ms	400 ms	50 ms	100 ms	200 ms	400 ms
A1	161	162	163	171	–	–	–	–
A2	155	155	155	162	–	–	–	–
A3	163	162	161	176	–	–	–	
B1	174	171	165	164	–	–	–	–
B2	158	124	75.7	63.6	2.03	1.20	0.57	0.33
B3	201	144	94.9	82.6	3.11	3.11	2.50	2.32
C1	263	128	82.6	71.0	2.91	2.64	1.96	1.65
C2	144	118	82.1	71.7	3.17	2.36	1.54	1.34
C3	205	173	116	101	2.87	2.70	1.74	1.96

[a] As calculated from the first four data points.
[b] As calculated from the last four data points.

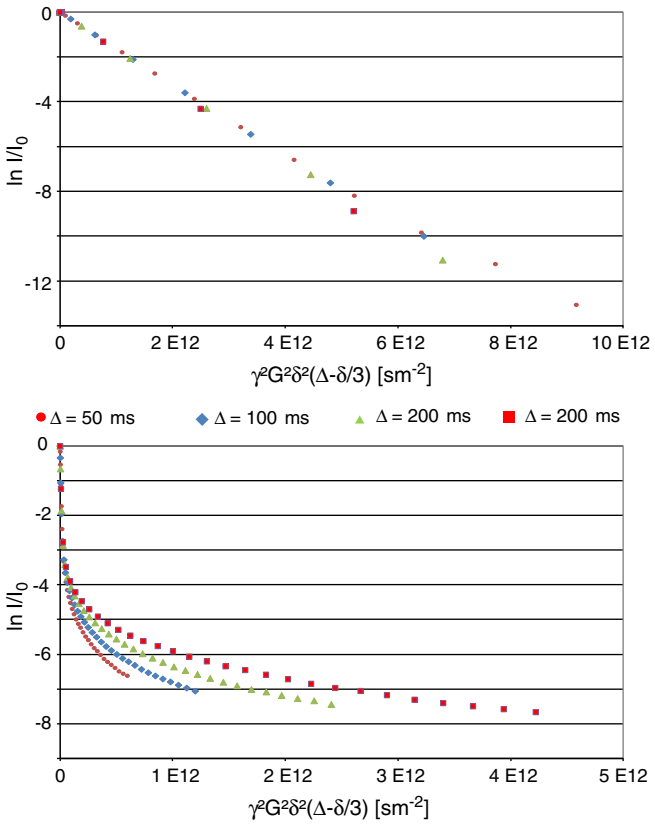

Fig. 8. PFG-NMR echo decay plots on PC in pure PG (top) and in a PG/water mixture 70:30 (bottom). In both cases, the PG signal at 1.150 ppm has been used for the analysis. Note the significantly different scales of the plots: the initial slopes of all plots are equal within the given experimental uncertainty.

is found next to a slow one, where the self-diffusion coefficient strongly scales with the pulse spacing Δ. The latter behavior, a roughly reciprocal dependence of the apparent self-diffusion coefficient D_{app} on Δ, is typical for a rapid and hindered diffusion in a small cavity [25].

Under these conditions, the size of the cavities can be calculated according to [25]:

$$D_{app} = \frac{R^2}{5\Delta}. \quad (2)$$

With the data for B2 from Table 4, this results in vesicle radii of 0.71 μm, 0.77 μm, 0.76 μm, and 0.81 μm, respectively. This corresponds to an average vesicle radius of 0.76 μm with standard deviation of 0.04 μm. For the PG/water ratio of 50:50 (sample B3), the self-diffusion coefficient shows only a weak dependence on Δ (Table 5). This indicates the growing contribution of the Brownian motion of the vesicles to D_{app} connected to the decreasing viscosity of the solvent and, possibly, to decreasing vesicle size.

3.10. Systems containing anionic phosphatidylcholine, samples C1, C2 and C3

Although the samples containing negatively charged PC were based on a PG/water ratio of 70:30, they behave similarly to the 50:50 sample B3. Regarding the slowly diffusing fraction of PG, the dependence of D_{app} on Δ does not follow the reciprocal law expected from Eq. (2). This may be explained by a reduced size of the vesicles such that their Brownian motion superimposes on the observed self-diffusion of the PG.

Table 5
Diffusion coefficients from PFG-NMR for the three sample series investigated at room temperature.
A1–A3: 1, 2 and 3% PC in PG; B1–B3: 3% PC in PG water mixtures 90:10, 70:30 and 50:50, resp.; C1–C3: 3% PC in 70% PG/30% water with 0.06, 0,12 and 0,3% of additional anionic phospholipid. The values for Δ denote the spacing between the two gradient pulses varied between 50 and 400 ms.

	Self diffusion coefficients (peak 4 of PG) in 10^{-12} m^2s^{-1}							
	Mobile fraction[a]				Immobile fraction[b]			
	50 ms	100 ms	200 ms	400 ms	50 ms	100 ms	200 ms	400 ms
A1	21.1	19.1	16.2	13.0	2.67	1.32	.676	.362
A2	18.5	17.3	15.0	12.2	2.42	1.21	.634	.337
A3	18.4	16.9	14.3	11.3	2.42	1.22	.645	.371
B1	15.7	12.7	10.0	7.56	2.08	1.17	.639	.352
B2	17.7	12.8	7.64	3.77	.854	.406	.203	.101
B3	52.9	41.0	30.7	21.4	.759	.302	.118	.005
C1	18.9	14.1	9.68	5.77	.913	.458	.226	.114
C2	21.7	16.6	11.9	7.31	.587	.302	.146	.0072
C3	31.1	24.0	17.6	11.9	.645	.293	.135	.0064

[a] As calculated from the first four data points.
[b] As calculated from the last four data points.

3.11. Results for the gels at room temperature

The large diffusion coefficients are about the same as the diffusion coefficients of the solvent in the PC-free fluid. Obviously, they refer to the free self diffusion in the continuous phase. The coefficients for the hindered diffusion are about an order of magnitude smaller than the coefficient for the free diffusion. The coefficients for the samples with water are smaller than without water. This could be an indication that the gels in the two types of systems have a different morphology, as has been found out by SAXS and cryo-TEM measurements.

It is noteworthy to mention that the values of the diffusion coefficients are about one order of magnitude smaller for the entrapped molecules than for the free molecules. The values for the entrapped molecules depend on the system composition. They are higher for the samples that contain no water than for the samples with water. This could be a consequence of the fact that the scaffolding of the flat bilayers is not being as dense for the diffusion as the compartments which are formed by the vesicles.

Alternatively, this could also indicate different compartment sizes. According to Eq. (2), one would obtain compartment radii of 0.8 ± 0.07 μm for samples A1, A2, A3, and B1. With 0.38 ± 0.08 μm, the values for the compartment radii would be significantly smaller for samples B2, B3, C1, C2 and C3.

The scaffolding network could perhaps look like a card house structure, in which the inner compartments are not completely closed, but have openings towards the continuous bulk phase.

3.12. Cryo-TEM

Previous measurements had shown already that it is difficult to obtain good cryo-TEM and FF-TEM of the PC-structures in the gels [2]. It is likely that the reason for this is, as in the case of visible light, that there is no contrast for the electrons between the bilayers and the solvent, when the refractive index of the bilayers is matched with the refractive index of the solvent [3]. Good Cryo-TEM micrographs could only be obtained when the gels were fractured mechanically and the solvent in the resulting pieces could be replaced with water. A micrograph obtained in this way is shown again in Fig. 9. The micrograph shows a large MLV, which consists of 5 vesicles inside each other. The interlamellar distance between the individual vesicles is however not constant, as is usually the case with vesicles in the liquid state. All the vesicles seem to be connected at one region of the MLV. It seems that a thin layer of solvent was between the bilayers, as can also be inferred from the SAXS.

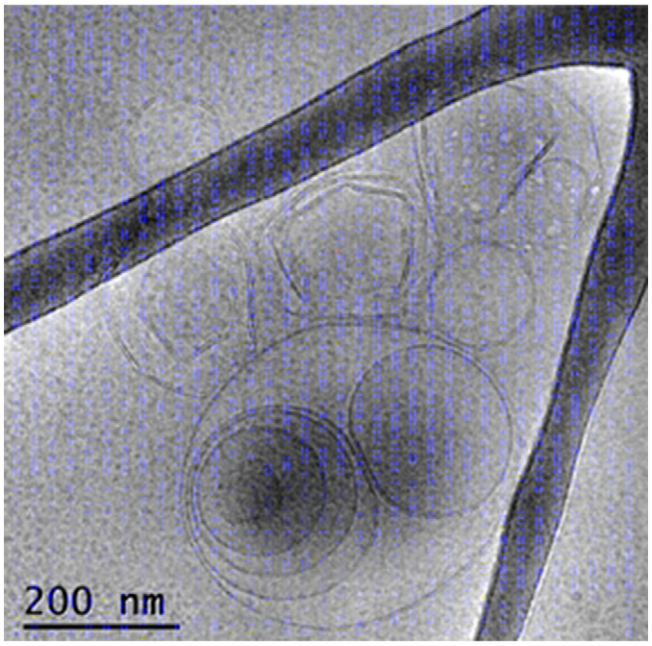

Fig. 9. Cryo-TEM of sample with 0.25% PC; prepared by dispersion of higher concentrated system into water.

A new TEM technique was used to study the structures in the gel samples with PC in the pure PG. With this technique it was possible to observe flat pieces of layers as shown in Fig. 10. The micrographs show only a weak contrast between the layers and the background. In view of what has been said before, the poor contrast makes sense. No vesicles could be observed in the samples without water. Actually this result is not surprising because the vesicles in the gel phase that contained additional water were a result of the vesicles which had already been present in the samples at 55 °C. On cooling the vesicles kept their identity but the bilayers were transformed into the crystalline state. In the samples without water no vesicles were present at 55 °C and no vesicles could therefore be present at room temperature. The observed flat crystalline pieces are obviously formed during cooling the

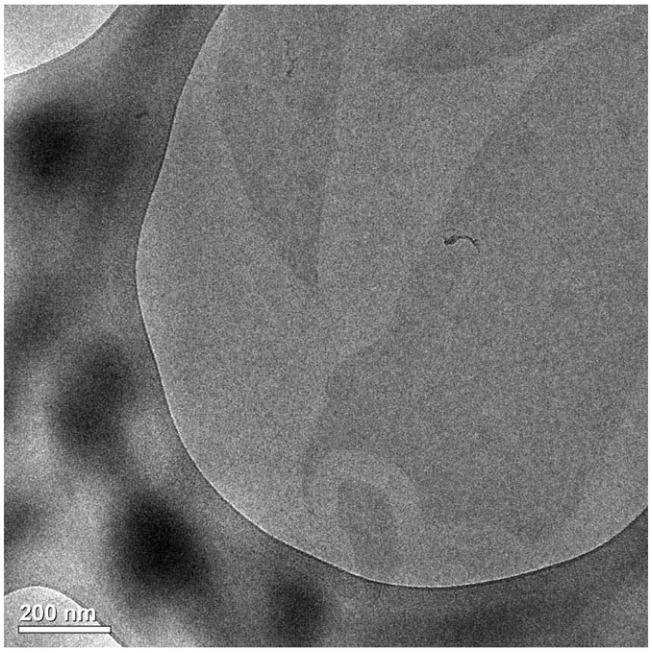

Fig. 10. Cryo-TEM of sample with 1% PC in PG.

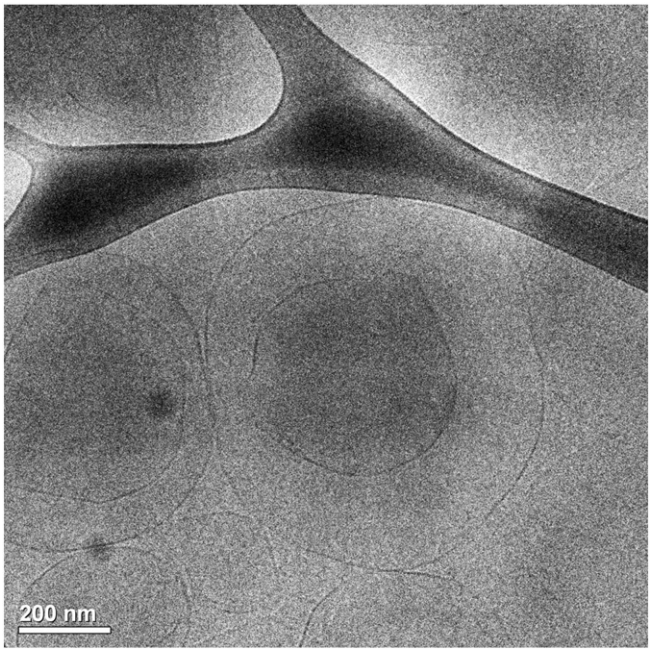

Fig. 11. Cryo-TEM of 3% PC in 50% PG + 50% water.

samples from high temperature to low temperature. When these pieces are formed they attract each other and form stacks of pieces. These stacks of aligned bilayers give rise to birefringence and to the scattering maxima at large q-values, representing repeat distances of around 4 nm. It is now also understandable why the scattering maxima are independent of the concentration of PC.

The distance to which the stacks can approach each other is independent of the concentration.

The stacks of the bilayers must also form a three dimensional structure that gives rise to the gel like properties of the samples. These clusters must have an inside and an outside, otherwise two different diffusion coefficients could not be observed in the samples.

With increasing water content in the solvent mixture it becomes easier to obtain good cryo-TEM micrographs. In Fig. 11a micrograph of a sample with 3% PC and 50% PG and 50% water is shown. Under these conditions the individual vesicles in the MLV have not yet collapsed to a single contact point as was the case in Fig. 9. Furthermore it is interesting to note that the entrapped vesicles are no longer of spherical shape. In most of them the bilayers seem to be facetted.

This is probably a result of the increased stiffness of the bilayers in the crystalline state. It is likely that during the crystallization process the bilayer of one vesicle develop crystalline flat patches, which become rapidly larger with time and then connect at different positions. The vesicles then look like vesicles when their concentration is above the critical concentration for dense packing, and their shapes are deformed. The situation is then similar as in emulsions when the droplets of the emulsion are deformed to a HIPE structure [26].

4. Conclusions

Dilute dispersions with particles of diacylphosphocholin (PC) swell to single L_α-phases with vesicles when co-solvents like glycerol, 1,3-butyleneglycol, or 1,2-propyleneglycol, or when mixtures of the two solvents are added to the aqueous dispersions. Surprisingly, the fluid L_α-phases for $T > T_m$ do not show Bragg-peaks at the expected q-values. The swelling of the PC-particles is due to the matching of the refractive index of the solvent with the refractive index of the bilayers. At the matching point, the attraction between the bilayers disappears and the bilayers are pushed apart by the undulation forces (Helfrich undulation).

The formed L_α-phases with MLV's form birefringent gels, when the samples are cooled below the Krafft-temperature of the PC. The gelation in samples is due to the two-dimensional crystallization of the PC molecules in the bilayers, and of the formation of a three dimensional network of the vesicles in the L_α-phase.

On crystallization of the PC in the bilayers, the stiffness of the bilayers is increased. As a consequence, the bilayers can no longer undulate and form adhesive contacts.

The bilayer contacts are visible both by SAXS and by Cryo-TEM measurements.

Gels are also formed in the pure PC solutions in PG, when the solutions are cooled from $T > T_m$ to $T < T_m$. Such solutions at $T > T_m$ do not contain micellar aggregates or vesicles. PG must therefore be considered a very good solvent for the PC, much better than water and still better than glycerol. Below T_m the PC molecules form crystalline flat plates, which then form a three-dimensional network.

PFG-NMR measurements indicate that two different types of solvent molecules exist in both types of gels. One type can diffuse freely in the samples while the other is entrapped in the crystalline vesicles, which slows down their diffusion by several orders of magnitude.

The gels are very brittle and they are irreversibly destroyed at a deformation of 1%.

It is hoped that these gels can be used for slow release applications of medical drugs. It is even conceivable that by adjusting the Krafft-temperature to 40 °C by the use of proper PC or by using mixtures of different PC the drugs can be released in cancer cells, which possibly have an increased temperature in the human body compared to normal cells.

References

[1] Helfrich W. Z Naturforsch 1978;A 33:305–15.
[2] Shinto K, Hoffmann H, Watanabe K, Teshigawara T. Colloid Polym Sci 2012;290(1):91–5.
[3] Yun Y, Hoffman H, Richter W, Talmon I, Makarsky E. J Phys Chem B 2007;111:6374–82.
[4] Beugin S, Gabrielle-Madelmont C, Paternostre M, Ollivon M, Lesieur S. Prog Colloid Polym Sci 1995;98:206–11.
[5] de la Maza A, Parra JL. Arch Biochem Biophys September 10 1995;322(1):167–73.
[6] de Haas KH, Blom C, van den Ende D, Duits MHG, Haveman B, Mellema J. Langmuir 1997;13:6658–68.
[7] Lipowsky R. Colloq Phys 1990;C7, 51(supp. 23).
[8] Kaler EW, Herrington KL, Murthy AK, Zasadzinski JA. J Phys Chem 1992;96:6698–707.
[9] Bellare JR, Davis HT, Scriven LE, Talmon Y. Controlled environment vitrification system: an improved sample preparation technique. J Electron Microsc Tech 1988;10:87–111.
[10] Danino D, Gupta R, Satyavolu J, Talmon Y. Direct Cryo-TEM imaging of phospholipid aggregates in soybean oil. J Colloid Interface Sci 2002;249:180–6.
[11] L. M., Eisenberg A. Langmuir 2009;25(24):13730–6.
[12] Emerson MF, Holtzer A. J Phys Chem September 1967;71(10):3320–30.
[13] Song A, Reizlein K, Hoffmann H. Prog Colloid Polym Sci 2008;134:111–9.
[14] Parsegian VA. Van der Waals forces. Cambridge, UK: Cambridge University Press; 2005.
[15] R. Strey, Habilitationsschrift, Göttingen 1992, S. 26.
[16] Diat O, Roux D, Nallet F. J Phys II Fr 1993;3:1427.
[17] Escalante J, Gradzielski M, Mortensen K, Hoffmann H. Langmuir 2000;16(23):8653.
[18] Berghausen J, Zipfel J, Lindner P, Richtering W. Europhys Lett 1998;43:683.
[19] Cevc G, Marsh D. Phospholipid bilayers: physical principles and models. New York: Wiley; 1989.
[20] http://msdssearch.dow.com/PublishedLiteratureDOWCOM/dh_0042/0901b80380042a9f.pdf?filepath=propyleneglycol/pdfs/noreg/117-01541…&fromPage=GetDoc.
[21] Zou A, Hoffmann H, Eastoe J, Glatter O. J Colloid Interface Sci 2007;316:723–9.
[22] Bergmeier M, Gradzielski M, Hoffmann H, Mortensen K. J Phys Chem B 1999;103:1605.
[23] Price WS. PFG-NMR as a tool for studying translational diffusion: Part 1. Basic theory. Concepts Magn Reson 1997;9:299–336. http://dx.doi.org/10.1002/(SICI)1099-0534(1997) 9:5<299::AID-CMR2>3.0.CO;2-Ü.
[24] Linders J, Mayer C, Sekine T, Hoffmann H. J Phys Chem B 2012;116:11459–65. http://dx.doi.org/10.1021/jp3046565.
[25] Kärger J, Fleischer G, Roland U. PFG NMR studies of anomalous diffusion. In: Kärger J, Heitjans P, Haberlandt R, editors. Diffusion of condensed matter. Wiesbaden: Vieweg; 1998. p. 144–68.
[26] Kizling J, Kronberg B, Eriksson JC. On the formation and stability of high internal phase o/w emulsions. Adv Colloid Interface Sci 2006;123–126:295–302.